Spatiotemporal effects in long rf-biased Josephson junctions: Chaotic transitions and intermittencies between dynamical attractors

L. E. Guerrero and M. Octavio
Centro de Física, Instituto Venezolano de Investigaciones Científicas, Apartado 21827, Caracas 1020 A, Venezuela and Facultad de Ciencias, Universidad Central de Venezuela, Apartado 21201, Caracas 1020 A, Venezuela
(Received 12 September 1988; revised manuscript received 3 April 1989)

We present an extensive numerical study of a long rf-biased Josephson junction in the presence of an applied magnetic field. We show the great complexity of the system and clarify some of the diverse spatiotemporal relationships that exist. At low values of the rf amplitude the spatial constraint succeeds in exciting an oscillating and localized pattern of solitonlike character. The dynamical response of this excitation as the forcing amplitude is increased allows us to observe three distinct intermittent phenomena: intermittency induced by interior crises, spatiotemporal intermittency between strange attractors, and tangentlike spatiotemporal intermittency. We also analyze at higher rf-bias amplitude a transition to a regime consisting of traveling waves with the spontaneous development of dc voltage which we interpret as being due to spatiotemporal chaos.

I. INTRODUCTION

The relationship between temporal chaos and spatiotemporal patterns in systems with many degrees of freedom has received a great deal of attention in recent years; this problem has been studied theoretically in nonlinear partial differential equations[1] and in coupled maps,[2] whereas experimental observations have been reported for some confined hydrodynamical systems such as Rayleigh-Bénard convection[3] and Taylor-Couette flow.[4]

In particular, systems modeled by the driven damped sine-Gordon equation have shown to be a fruitful test field for these studies; these systems present the coexistence of the two main and extreme nonlinear phenomena: temporal chaotic dynamics and solitonic structures.[5–20] Furthermore, the sine-Gordon equation is ubiquitous in condensed-matter theory[21] because it is a simple wave equation involving a periodic local-potential term.

The tendency of a sine-Gordon-like system to preserve an initial solitonic state has been known for a few years,[6,8] while spontaneous pattern formation in them is a more recent preoccupation.[14,16,17,19] In particular, pattern formation and conversion in long Josephson junction (LJJ), which is a sine-Gordon-like system, appear to be a source of new spatiotemporal phenomena and provide a field in which simulation[17,19] and experiment[22] may act interactively. In addition, since the LJJ is fairly well understood, it may allow us to understand and describe better the origin of chaotic dynamics in this system.

In this paper we show that the solitonlike character of the LJJ can play a fundamental role as an activating mechanism of chaos and introduces a rich variety of new and interesting spatiotemporal phenomena. This is done by selecting a typical sequence of solutions with increasing rf bias, with parameters similar to those that can be achieved experimentally.

We show that, at very low values of the rf amplitude ($\rho < 0.380$), the chaotic dynamics of the LJJ are reminiscent of those exhibited by typical low-dimensional systems such as the Josephson junction without spatial extent. However, this does not mean that for the same values of dissipation, amplitude, and frequency of the forcing, both the Josephson junction without spatial extent and the LJJ exhibit identical responses. We show that in contrast with small Josephson junctions, which at low values of the rf amplitude only exhibit period one solutions,[23] the LJJ in the presence of an applied magnetic field exhibits quite a rich dynamical behavior in this regime. This is possible because, due to the boundary conditions and forcing, the system can generate localized oscillations of solitonlike character, which can be chaotic or subharmonic depending on the junction parameters. The development of a solitonic structure supposes the organization of the energy exchange in such a manner that only a few modes of the system participate effectively in the dynamics, leading to low-dimensional chaos despite the large number of degrees of freedom of the system.

We show for higher amplitudes ($\rho \geq 0.380$), that higher-dimensional effects can introduce spatiotemporal effects which can sensibly modify the usual chaotic scenarios. At $\rho = 0.380$, we find intermittency between strange attractors, which has spatiotemporal origin. Further increase of the amplitude of the forcing ($\rho = 0.65$) causes the appearance of a spatiotemporal tangentlike intermittency characterized by switching between two states corresponding to the loss and recovery of the solitonic character of the solution.

Finally, at large values of the amplitude of the rf bias ($\rho > 0.7375$), we describe a transition to a spatiotemporal chaotic traveling-wave regime; this transition corresponds to the *fluxonic regime* in which the LJJ develops an average voltage. This fluxonic regime is found to alternate with a localized wave mode that in addition to n periodicity can also exhibit two-frequency quasiperiodicity.[19]

Our paper is organized as follows. In Sec. II we present a description of our model and simulation. In Sec. III we present the study of the three different intermittency phenomena found: interior crises induced intermittency, intermittency between strange attractors, and spatiotemporal tangentlike intermittency. In Sec. IV the transitions between the spatiotemporal chaotic traveling-wave regime and the localized and oscillating wave regime are presented. Finally, in Sec. V we summarize and present our conclusions.

II. THE PHYSICAL MODEL AND ITS SIMULATION

A Josephson junction is considered to be long when its length is greater than the Josephson penetration depth λ_J; this implies that magnetic flux can now penetrate the insulating barrier and spatial effects can no longer be neglected.

This situation can be modeled by the following sine-Gordon-like equation[24,25] which assumes that the junction is effectively current biased by an rf drive (uniform in space) and shunted by an effective normal resistance R_N and an effective capacitance C,

$$-\frac{\hbar c^2 L}{8\pi e d}\frac{\partial^2\phi}{\partial X^2}+\frac{\hbar C}{2e}\frac{\partial^2\phi}{\partial T^2}+I_c\sin\phi = -\frac{\hbar}{2eR_N}\frac{\partial\phi}{\partial T}+I_{\rm rf}\sin(\omega_d T)\ , \quad (1)$$

where $\phi=\phi(X,T)$ is the phase difference of the superconducting order parameter between each side of the barrier, L is the length of the junction, d is the magnetic thickness of the junction, $I_{\rm rf}$ is the rf current, the term in $\partial\phi/\partial T$ represents quasiparticle loss, and I_c is the critical current. This equation can be reduced to a single dimensionless form

$$-\frac{\partial^2\phi}{\partial x^2}+\frac{\partial^2\phi}{\partial t^2}+\sin\phi=-\frac{1}{\sqrt{\beta_c}}\frac{\partial\phi}{\partial t}+\rho\sin(\Omega_d t)\ . \quad (2a)$$

Here the distance is normalized to the Josephson penetration depth $\lambda_J=(\hbar c^2 L/8\pi e d I_c)^{1/2}$, time is normalized to the inverse of the Josephson plasma frequency, $\omega_p=(2eI_c/\hbar C)^{1/2}$, and the rf amplitude ρ is normalized to the critical current I_c; $\beta_c=2eI_cR_N^2C/\hbar$ is the Stewart-McCumber parameter (a measure of the damping of the system) and Ω_d is the normalized applied frequency.

In order to take into account the presence of an external applied field, we use the following boundary conditions:

$$\frac{\partial\phi(0,t)}{\partial x}=\frac{\partial\phi(L,t)}{\partial x}=\eta\propto H(y)\ . \quad (2b)$$

Here H is the applied magnetic field normal to the surface of the insulating barrier. Thus the dimensionless quantity η in Eq. 2(b) is a measure of the external magnetic field.

The derivative in time of the phase difference is the voltage across the junction according to the Josephson relation

$$\hbar\frac{\partial\phi}{\partial T}=2\ \text{eV}\ , \quad (3)$$

where T is the unnormalized time.

The LJJ can support coherent and persistent spatiotemporal excitations, i.e., solitonlike states, because of the underlying sine-Gordon nature of the system. For instance, the solitonic traveling-wave excitation in a Josephson junction is a current loop (composed of surface current and tunneling supercurrent) connecting the two surface layers via the barrier. This current loop encompasses one quantum of magnetic flux Φ_0 and the solitonlike excitation is therefore often called a *fluxon*. From the integration of Eq. (3), a time-averaged voltage corresponds to the presence of a time-averaged magnetic flux. The ability of the system to support fluxons or solitonic traveling waves requires a threshold energy just like the kink solutions of the pure sine-Gordon equation.

Other fundamental nonlinear normal modes of the sine-Gordon equation that are found in the LJJ system are the *breather* and *plasmon* oscillations; in contrast to kinks, both of these solutions do not require a threshold energy, i.e., they can be sustained even for low input energies.

The breather oscillation is a solitonlike state with an internal degree of freedom, which can be regarded as formed by a bounded kink-antikink pair (i.e., fluxon-antifluxon pair in the LJJ case[25]) whereas the plasmon oscillations are noncoherent, small-amplitude harmonic solutions.

In all the results to be presented in this paper, the parameter values are $L=5$, $\beta_c=15.744$, $\eta=1.25$, and $\Omega_d=0.65$. The choice of these parameters corresponds to realistic values, like those that can be obtained in the laboratory. At the same time we have studied these parameters in detail because, for increasing rf bias, they exhibited a rich variety of the solutions that can be found in various regions of parameter space. Similarly, the high damping prevents the spurious generation of plasmons without the need for special initial conditions which cannot be obtained in experiments.

We have integrated system (2) using a standard implicit finite-difference method dividing the junction into 128 sections. Because we stress our interest in spontaneous pattern formation, our integration was started from flat initial conditions $\phi(x,0)=0$ at all points but at the ends where we forced the system to satisfy the boundary conditions. Unless otherwise stated we plot variables only at the center of the junction.

A mechanical analog of the system under consideration is a chain of coupled pendula in the presence of damping and forcing. This chain of pendula can be modeled by a system such as (2) in which the term ϕ_{xx} represents the interaction between pendula and η represents an applied torque at the extremes of the chain.

III. LOW-ENERGY BREATHER REGIME

At values of the rf amplitude below the threshold for fluxon generation ($\rho<0.7375$), the LJJ generates a localized breatherlike excitation whose frequency can match the one of the drive or some subharmonic of it, as well as

produce a chaotic response. This regime is of interest for a variety of reasons. First, there are qualitative changes, due to the spatial variable, to the usual chaotic scenarios. Second, new spatiotemporal phenomena can also appear. Also, in contrast with the LJJ, the junction without spatial extent can only exhibit period-1 solutions in this limit.[23] In this section we describe these phenomena.

A. Scenario of interior crises

In this section we describe the generation of a breatherlike excitation in the low-energy regime and detail how its temporal response evolves through a period-doubling cascade and an internal crises sequence. We also point out the similarities and differences of this last chaotic scenario with respect to those already known for low-dimensional systems.

The presence of the applied magnetic field induces symmetry breaking which in turn leads to the excitation of an oscillating and localized spatial structure, which can interact strongly with the driving force. This is similar to the case of the temperature difference and external forcing in Rayleigh-Bénard convection another continuous and dissipative system that exhibits low-dimensional chaos and organization of localized and traveling patterns.

At low energies the junction exhibits no average voltage and, therefore, zero-time-averaged magnetic flux is present. This situation corresponds in the mechanical analog of the LJJ to each of the "coupled pendula" being trapped in one well of its own periodic potential ($-\pi<\phi<\pi$).

We have verified that all the spatial points of the junction present the same kind of dynamical attractor in this regime. While the qualitative similarity of the dynamics at every point is guaranteed by the existence of a solitonic profile, from point to point the phase-space plots (ϕ_t versus ϕ) are found to vary their detailed shape. This asymmetry of the response is also introduced into the system by the applied magnetic field.

As ρ is increased, a solitonic structure of the breather type is found up to $\rho=0.34$, when it enters a period-doubling cascade. As ρ is increased even further, a chaotic response is eventually attained but the solitonic character of the response persists. That is, the breather is still present but now its oscillation is nonperiodic. The dynamical attractor for this solution is found to be like those characteristic of low-dimensional systems, despite the large number of degrees of freedom of the LJJ.

The low-dimensional character of this strange attractor can be specified even further. In fact, it corresponds to an *interior crisis*, as shown in Figs. 1 and 2. We recall that in the literature[26] a *crisis* is defined as a certain sudden change of the strange attractors that occurs when the control parameter of the experience is varied. An interior crisis is one that preserves the boundary of the basin of attraction; these events are the result of the collision of an unstable periodic orbit with a strange attractor.

In Fig. 1 ($\rho=0.3530$) we present the strobed time series for the voltage ϕ_t in which the value of the voltage is plotted at each period of the forcing. Note that the

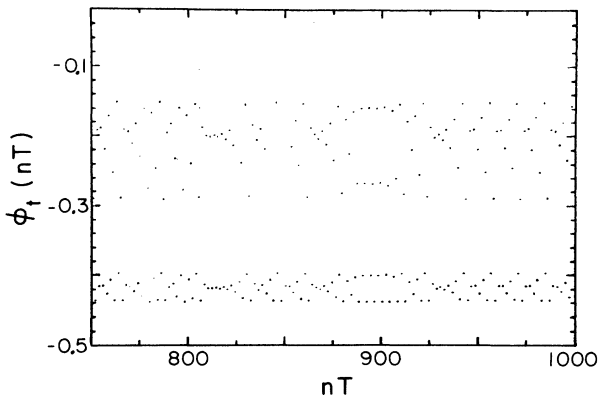

FIG. 1. Intermittency induced by interior crisis. The strobed time series $\phi_t(nT)$ vs nT for $\rho=0.3530$ reveals a two-band chaotic regime with occasional $2n$-periodic windows.

system shows occasional windows in which the system is in a period-2 or -4 state, embedded in the aperiodic or chaotic bands. In order to demonstrate that this corresponds to an interior crisis, one has to resort to plotting the return map for the fourth iterate, $\phi((n+4)T)$ versus $\phi(nT)$, which would reveal the presence of unstable period-2 and -4 solutions. It is known[27] that in the Nth iterate return map a periodic orbit is stable only in the case that the absolute value of its derivative at the intercepting point with the line $\phi((n+N)T)=\phi(nT)$ does not exceed unity. Because of this, in order to search for the possible coexistence of unstable periodic attractors together with the chaotic attractor, we must construct the

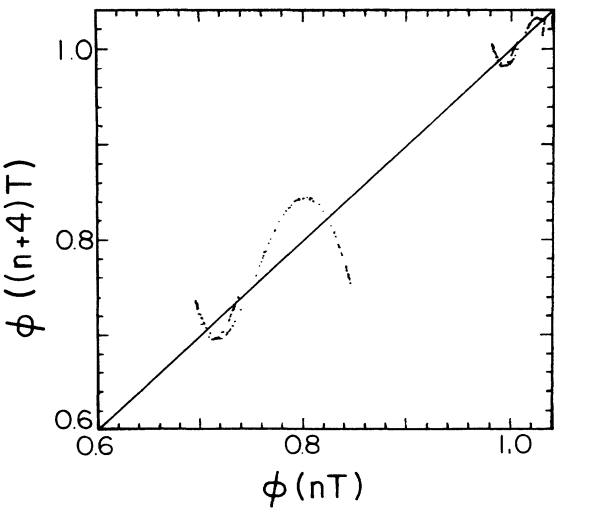

FIG. 2. Interior crisis. The return map for the fourth iterate $\phi((n+4)T)$ vs $\phi(nT)$ at the threshold of the fusion of four bands into two, evidences the coexistence of a four-piece strange attractor and at least an unstable period-4 and an unstable period-2 orbit.

return map for the fourth iterate, $\phi((n+4)T)$ versus $\phi(nT)$.

In Fig. 2 we show such a return map for the fourth iterate, $\phi((n+4)T)$ versus $\phi(nT)$, at the threshold of the fusion of four bands into two. This map exhibits four pieces, each one intercepting the line $\phi((n+4)T) = \phi(nT)$ with a slope of absolute value exceeding one. In addition, one can also identify the emergence of another two intercepts with a slope of absolute value exceeding one at the points where each pair of pieces is fusing. Therefore, Fig. 2 shows the coexistence of a four-piece strange attractor and at least an unstable period-4 orbit and an unstable period-2 orbit that have successively collided with the nonconnected strange attractor as the pieces merged. This shows that once a nonconnected chaotic attractor has been attained via period doubling, the attractor evolves through successive interior crises which reduce the number of its disconnected pieces.

In the case of the junction without spatial extent, numerical and analog simulations have shown different types of crises,[28–34] particularly, the broadening of bands and the nonconnected strange attractors have been previously reported. These last couple of phenomena have also been observed experimentally in the nonlinear and forced semiconductor oscillator.[35–39]

Both the junction without spatial extent and the semiconductor oscillator are systems whose dynamics are only temporal due to their low dimensionality as well as certain mathematical models[26] (for example, the logistic equation) that also exhibits the occurrence of a bifurcation cascade followed by a succession of interior crises. Therefore, the occurrence of this phenomenon in the LJJ is not wholly unexpected, is not ascribable to its spatial extent, and simply reflects the possibility of low-dimensional behavior in the system. That such is the case is shown in Fig. 3 where we present the return map for the two-piece attractor and two-band chaos ($\rho=0.3530$). In this return map the different pieces exhibit low dimensionality, indicative of the few degrees of freedom effectively involved in the dynamics.

Indeed there is a close relationship of the two-piece return map of Fig. 3 with that already known for other models and systems with just one degree of freedom: one of the pieces that composes the map has a parabolic shape similar to the return map generated by the logistic equation while the other piece has a close resemblance to the return maps obtained[40–42] for the forced diode and the discrete map that models it, as well as for spin-wave instabilities forced by microwave fields.[43]

While this crisis is quite similar to that reported previously in other systems, there is one point in which the intermittency induced by the crisis scenario presented for the LJJ differs: we have not observed the presence of a response with the $(1/f)^d$ spectrum at low values of frequency. This type of behavior is usually associated with intermittency between dynamical attractors.[32,34]

If the bias amplitude is increased even further, the sequence of interior crisis is interrupted when the two pieces of the strange attractor attempt to fuse via the collision with an unstable period-1 attractor. In this regard, the two-piece strange attractor also suffers a crisis, but of a different kind. This time the region of attraction is sensibly enlarged for brief periods of time, as can be appreciated in the strobed time series of Fig. 4 ($\rho=0.354$). The enlargement of the region of the attraction supposes the sudden removal of the boundary of the former basin of attraction at the moment when the line $\phi((n+1)T) = \phi(nT)$ in the return map is crossed. The corresponding strange attractor (Fig. 5) not only occupies a larger region of the Poincaré map, but also exhibits a well-defined fractality. This reveals that the system is still behaving as a low-dimensional one.

We would like to define this event to be a new type of crisis: it cannot be regarded as an interior crisis because

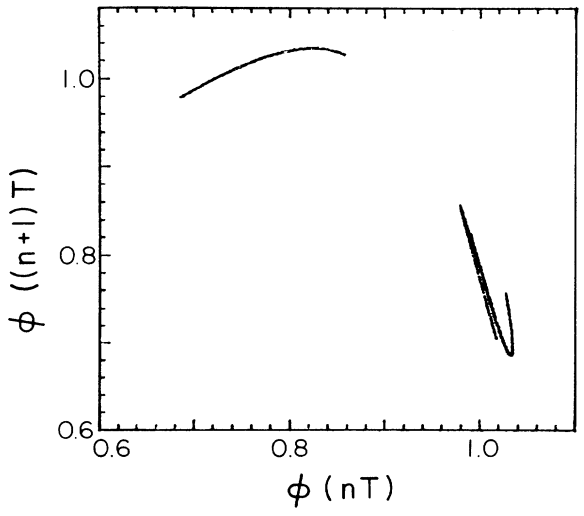

FIG. 3. Interior crisis. Return map for the two-piece attractor and two-band chaos ($\rho=0.3530$). In this return map the different pieces exhibit low dimensionality which is indicative of the few degrees of freedom which are effectively involved in this dynamics.

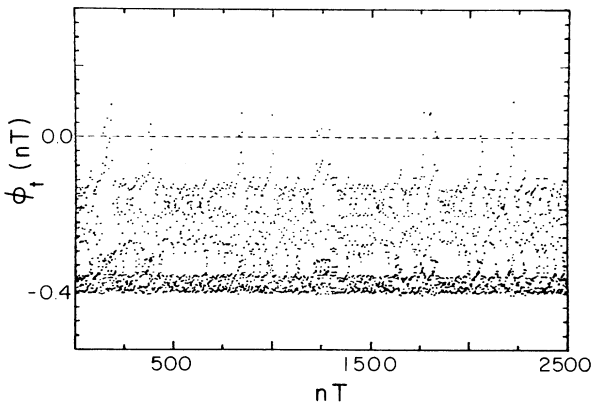

FIG. 4. *Strange attractor boundary crisis.* Strobed time series $\phi_t(nT)$ vs nT for $\rho=0.354$ reveals a sensibly enlargement of the region of attraction when the two pieces of the strange attractor attempt to fuse via the collision with an unstable period-1 attractor.

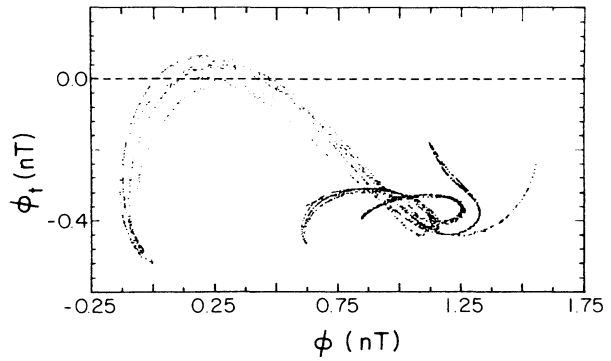

FIG. 5. Poincaré map $\phi_t(nT)$ vs $\phi(nT)$: low-dimensional chaotic behavior after the *strange attractor boundary crisis* ($\rho=0.375$).

of the sensitive enlargement of the previous basin of attraction; neither can this event be identified as a *boundary* crisis[26] because, after the collision with the unstable period-1 orbit, the former strange attractor has been replaced by another strange attractor, and not by a periodic orbit as is usually the case. Therefore we would like to call it a *strange attractor boundary* crisis. This new kind of crisis is a transition between two low-dimensional-like regimes similar to that exhibited by small junctions and cannot be related to the fact that the junction is now larger than its penetration depth.

B. Scenario of spatiotemporal intermittency between strange attractors

Hereafter we will present a new kind of crisis in which spatial effects are partially responsible for the dynamic transition. As a result of this event, an intermittent regime between two strange attractors can be spontaneously attained by the system.

The chaotic dynamics [which we have already presented in Fig. 5 (Poincaré map)] for $\rho=0.375$ suddenly change at $\rho=0.380$ to the one shown in Fig. 6 (note the different scales between them). This dynamical transition suddenly enlarges the basin or region of attraction and increases the dimension of the corresponding strange attractor that rules the system (compare the Poincaré maps 5 and 6).

The involvement of the spatial variable in the genesis of the phenomenon can be proved by noting that the Poincaré map of Fig. 6 ($\rho=0.380$) is the superposition of the maps for $\rho=0.375$ in the case of a junction of length $L=5.0$ (Fig. 5) and that of the one with $L=4.0$ (Fig. 7).

Thus this dynamical transition can be regarded as a *spatial crisis* due to the sudden removal of the boundary between the basin of attraction for the junction of length $L=5.0$ and the basin of attraction for the junction with length $L=4.0$, i.e., the two strange attractors now share the same basin of attraction. A crisislike dynamical transition, which originates on the existence of the spatial extent of the system, has not been previously known and shows how spatial effects contribute and are an integral part of the complexity of dynamical systems with spatial extent.

The difference of the phase between two points of the barrier (the middle and an extreme), taken at each period of the forcing, corresponding to the overlapped strange attractors, is presented in Fig. 8. In this plot it can be seen how much time the system spends in each of the coexisting attractors, while it also reveals the spatial dependence of the junction phase (i.e., the inhomogeneous character of the alternate solutions). This clearly shows that this regime is a *spatial intermittency* between the two strange attractors which the system has for two different lengths.

The strobed difference of the phase series of Fig. 8 is analogous to the strobed time series reported in the case of the junction without spatial extent[28] for intermittency between strange attractors *induced by noise.* This last phenomenon is known as multistability.[45–47] It is necessary to point out that the phenomenon we are reporting is the only known case in which two strange attractors

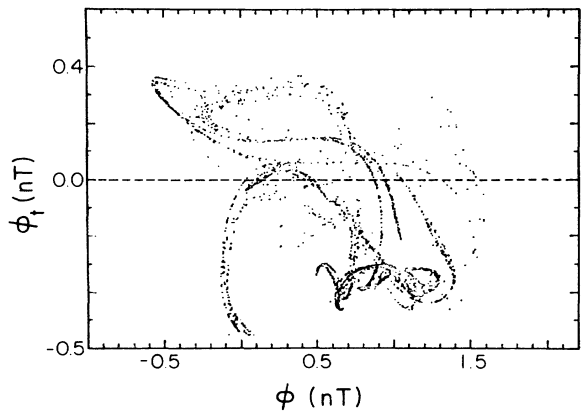

FIG. 6. *Spatial crisis* ($\rho=0.380$). Poincaré map $\phi_t(nT)$ vs $\phi(nT)$ shows the increasing of the dimension of the attractor and reveals an enlargement of the basin or region of attraction. Note the different scales in 5 and 6.

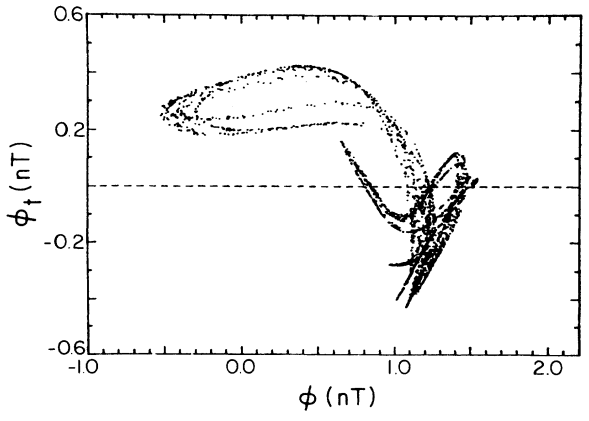

FIG. 7. *Spatial crisis.* The Poincaré map of Fig. 6 is the superposition of the maps for $\rho=0.375$, in the case of a junction of length $L=5.0$ (Fig. 5) and the map of one with $L=4.0$ (Fig. 7).

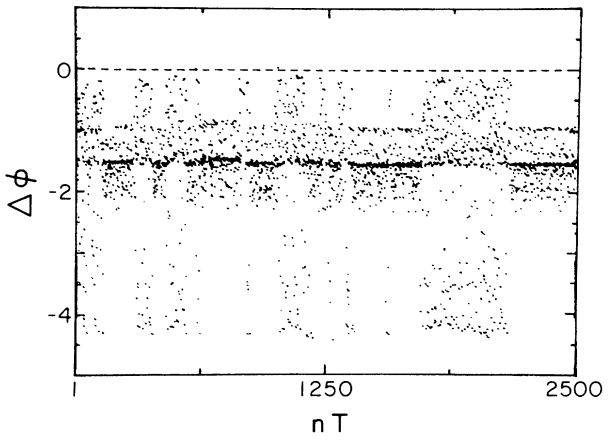

FIG. 8. Spatial crisis. The difference of the phase between two points of the barrier (the middle and an extreme), taken at each period of the forcing, $\Delta\phi(nT)$ vs nT, corresponding to the overlapped strange attractors reveals how much time is expended for the dynamics ruled by each one of the coexisting attractors, while also revealing the spatial dependence of the junction phase (i.e., the inhomogeneous character of the alternate solutions).

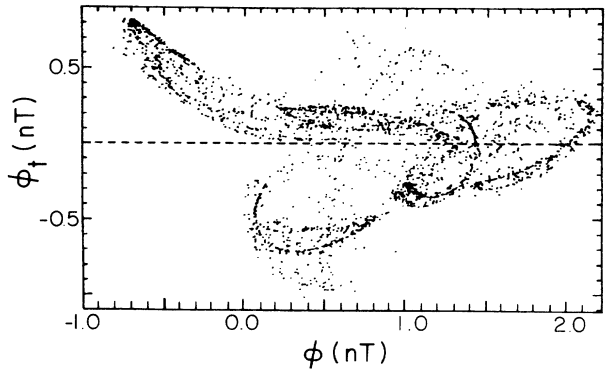

FIG. 9. Activation of an increased number of effective degrees of freedom ($\rho=0.5$). Poincaré map $\phi_t(nT)$ vs $\phi(nT)$ exhibits a loss of fractality of the dynamical attractor.

collide or coexist *without* the presence of noise inducing the instability of the attractors. This spontaneous character raises the novelty and importance of this spatiotemporal dynamic transition; furthermore, other noninduced phenomena of coexistence or collision of attractors (such as interior and external crises and temporal intermittency) involve a strange attractor and a periodic one; never, as far as we know, two strange attractors.

A possible physical explanation of the instability of the strange attractors involved in the spatial intermittency between two chaotic regimes may be that both of the breather profiles corresponding to each one of these chaotic attractors are incommensurable with the spatial length of the junction which makes it unstable; this causes the system to attempt to find a stable condition, but the other nearby attractor is also unstable. In the case of the LJJ, the intermittency between the two strange attractors does not generate $(1/f)^d$ noise (at low frequencies), in contrast to the case of intermittency between two strange attractors induced by noise.

C. Scenario of spatiotemporal tangentlike intermittency

The subsequent increase of the rf-bias amplitude determines the appearance of a high-dimensional chaotic regime which appears to originate by disorder in the spatial degrees of freedom.

We introduce this new kind of effect by presenting the Poincaré map (Fig. 9) at $\rho=0.5$; at this value of the rf bias the amplitude of the oscillations in phase space increases significantly and the identities of the formerly overlapped attractors are no longer distinguishable.

This strange attractor exhibits a definite loss of fractality; this increase of the dimension of the chaos can be assumed to be due to the spatial variable: the higher dimensionality of the Poincaré map indicates a relaxation of the solitonic character of the solution caused by the activation of an increased number of effective degrees of freedom and a consequent breaking of the order in the energy exchange between the different modes.

This regime is followed by an intermittency between two spatially inhomogeneous regimes characterized in time by period-3 and high-dimensional chaos, as shown in Fig. 10(a), which plots the difference of the phase between two points of the barrier (the middle and an extreme), taken at each period of the forcing for $\rho=0.65$.

The third iterate of the return map $\phi((n+3)T)$ versus $\phi(nT)$, Fig. 10(b), presents three regions of high concentration of points that approaches in tangentlike fashion the line $\phi((n+3)T)=\phi(nT)$, where periodic solutions exist. In this respect the map resembles the usual one for the *intermittent transition to chaos or tangentlike bifurcation,* but, in addition, the map also exhibits an increased dimensionality which reflects the occasional spatiotemporal disorder. The power spectrum analysis again reveals an absence of $(1/f)^d$ decay at low frequencies; this fact contrasts with the usual association between this kind of noise and the tangentlike intermittent route to chaos.[44]

Figure 10(c) shows the corresponding phase-space portrait which reveals the underlying mechanism: each one of the "pendula" that forms the mechanical analog has reached sufficient energy as to explore the more nonlinear region of the potential well in which it is trapped and even to visit the adjacent wells. The sensitivity to the initial conditions increases its importance because near the maximum of the potential there is more sensitivity to where the trajectory ends; this provokes a loss of the coherence of the solution, i.e., the breather is destroyed. This event corresponds to the high-dimensional chaos, whereas the reconstruction of the solitonic profile corresponds to the period-3 response.

Spatiotemporal intermittency with loss of the solitonic character of the solution has been previously reported for the nonlinear Schrödinger equation[48] among other partial differential equations;[49] in addition, the transition to spatiotemporal intermittency has been experimentally stud-

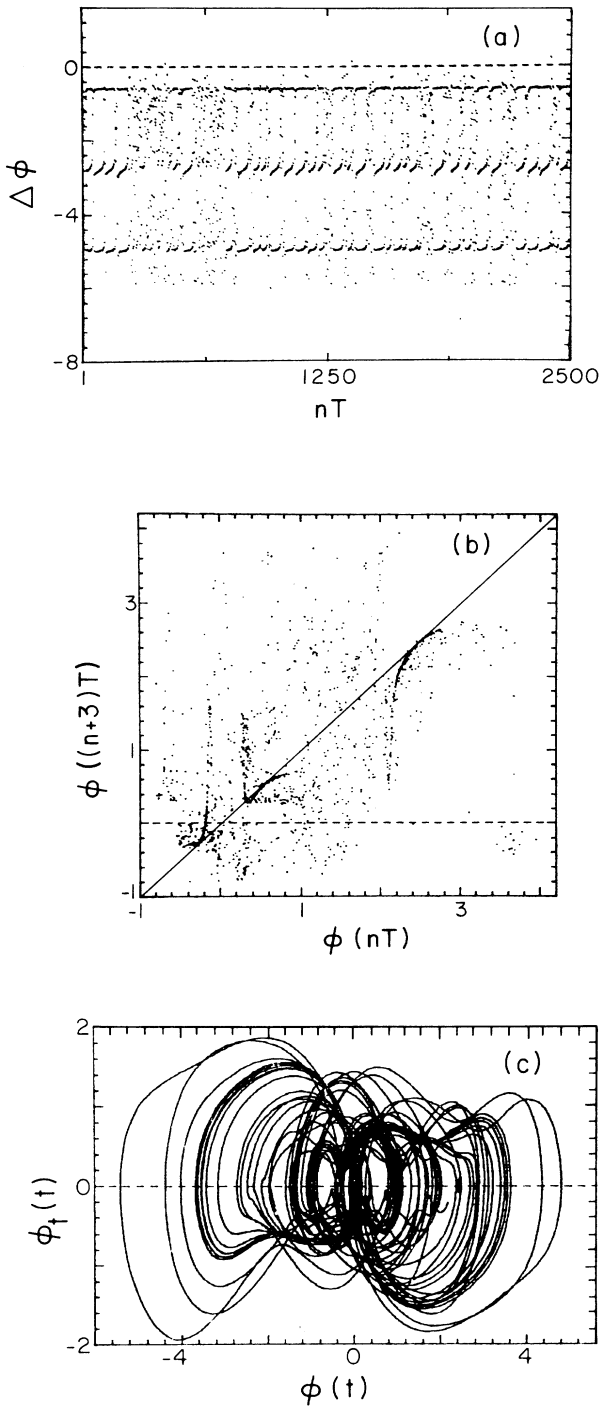

FIG. 10. Spatiotemporal tangentlike intermittency ($\rho=0.65$). (a) The difference of the phase between two points of the barrier (the middle and an extreme), taken at each period of the forcing, $\Delta\phi(nT)$ vs nT, reveals an intermittency between two spatially inhomogeneous regimes characterized in time by period-3 and chaos. (b) The third iterate of the return map $\phi((n+3)T)$ vs $\phi(nT)$ presents three regions of high concentration of points that approach in tangentlike fashion the line $\phi((n+3)T)=\phi(nT)$. (c) Phase space $\phi_t(t)$ vs $\phi(t)$ showing trapped solution attempting to visit the adjacent wells of the potential.

ied in Rayleigh-Bénard convection.[50] Nevertheless, we point out that a clear identification of a dynamical transition of spatiotemporal character as a tangent bifurcation [as the third iterate of the return map $\phi((n+3)T)$ versus $\phi(nT)$ reveals at Fig. 10(b)] had not been previously demonstrated.

As the rf-bias amplitude is increased even further, the characteristic stability of the solitons is the prevailing effect and for $\rho=0.7$ the system sustains a period 3 breather trapped in three wells of the potential, not in one well, as in the case of all the dynamics presented earlier. The system visits the adjacent potential wells while preserving the breather's spatiotemporal pattern, in contrast to the former tangentlike intermittent regime.

IV. REGIME ABOVE THE THRESHOLD FOR THE FLUXON GENERATION

A. Fluxonic regime

In this section we present results for rf-bias amplitudes of the forcing above the fluxonic threshold ($\rho>0.7375$); in this range of parameters the onset of chaos is associated with an increase of the equipartition and the exchange of the energy between the modes, because the dynamical behavior corresponds to the regime of creation and destruction of fluxons.

At $\rho=0.7375$ the system has sufficient energy so that the breather excitation suddenly splits into two traveling waves which propagate in opposite directions (a fluxon and an antifluxon).[5,25,51] For our choice of the value of the applied magnetic field ($\eta=1.25$), numerical and experimental studies show that the incoming fluxons are annihilated into plasma oscillations at one end of the junction.[52,53] The plasmons then travel back to the other end of the junction and trigger a new fluxon and in this way a process of alternate creation and destruction of fluxons is established.

Figure 11 presents the Poincaré map for the direct

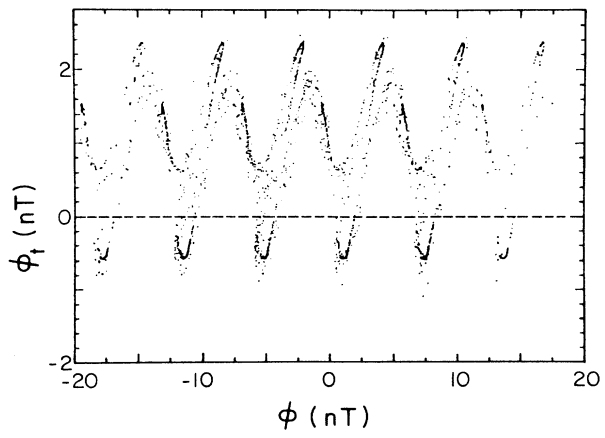

FIG. 11. Fluxonic regime ($\rho=0.7375$). Poincaré map $\phi_t(nT)$ vs $\phi(nT)$ for the direct transition from localized oscillations of period-3 to chaotic traveling waves; solutions diffuse from one well to another.

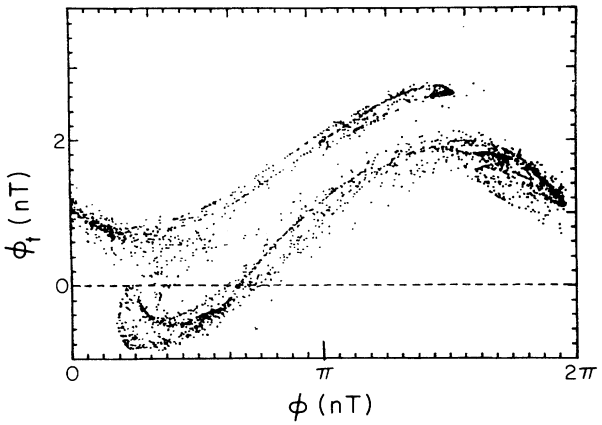

FIG. 12. Fluxonic regime ($\rho=0.7375$). Poincaré map $\phi_t(nT)$ vs $\phi(nT)$ (mod 2π) showing a strange attractor with a loss of its fractality because the presence of the plasmons implies the activation of an increased number of degrees of freedom.

transition from localized oscillations of period-3 to chaotic traveling waves; in this figure traces of the period-3 attractor still appear. As can be appreciated in Fig. 11, solutions in this regime diffuse from one well to another; these kinds of solutions are known as free-running solutions. This situation amounts in the mechanical analog to the possibility of the pendula performing complete revolutions. Due to the propagation of excitations the system exhibits a finite voltage, as shown by the zero-frequency peak at the power spectrum; thus it follows from Eq. (4) that the insulating barrier holds magnetic flux quanta in the time average.

Figure 12 corresponds to the same solution as Fig. 11 and it presents the Poincaré map (mod 2π); this figure reveals a strange attractor with a loss of its fractality because the presence of the plasmons implies the activation of an increased number of degrees of freedom. The presence of nonsolitonic excitations introduces disorder into the energy exchange. Recently a similar transition from localized oscillations to a traveling-wave regime has been reported for the Rayleigh-Bénard convection.[54]

B. Boundary crisis: fluxon annihilation

In this section we present a dynamical transition which results in the existence of breatherlike solutions even above the fluxonic threshold.

Due to the dissipative nature of the LJJ, the fluxons are not perfectly solitonic excitations; thus they can exchange energy in collisions between them or with plasmons. In addition, it is known that these collisions also produce radiation emission.[55] It has been predicted by theory[25,55] that these characteristics of the collisions in the fluxonic regime can lead to the annihilation of the fluxons and plasmons into a breather excitation. Recently this phenomenon has been detected by experiment.[22]

In what follows we show that this annihilation process in the LJJ can be identified as an *external or boundary crisis.*[26] An external crisis is a collision of a strange attractor with a periodic orbit which produces the destruction of the basin of attraction of the chaotic attractor and the replacement of the chaotic attractor by a periodic attractor; the event is characterized by the occurrence of a *chaotic transient* in which the dynamics is determined for a period of time by the chaotic attractor which is eventually destroyed.

The strobed time series of Fig. 13 presents the chaotic transient associated with the boundary crisis for an amplitude of the rf bias $\rho=0.8$. In this case the transient is remarkably long: almost 3000 periods of the driving force.

Kautz[56] has obtained a similar noise-free crisis event for the junction without spatial extent. Our result also occurs in the absence of disordered input of temperature, but in addition, because of the presence of the spatial variable, it also exhibits the transition from traveling waves to a localized oscillation.

In previous work[19] we have shown that, in contrast to the breather excitations at low values of the rf bias, this time the breathers can exhibit, in addition to n periodicity and chaos, spontaneous generation of quasiperiodic behavior which arises from the competition between two incommensurate frequencies: one due to the driving force and the second one due to the oscillation of the breather at its natural frequency.

This breather regime is again localized in space and eventually becomes unstable and changes into a new traveling-wave regime, establishing, as the amplitude of the forcing is increased, a switching regime between a free-running solution involving an increased number of fluxons and a trapped solution in an increased number of wells of the potential. As an example, Fig. 14 presents at $\rho=2.625$ a trapped quasiperiodic solution in three wells of the potential.

The spontaneously generated quasiperiodic behavior of the LJJ is quite similar to that of the Rayleigh-Bénard convection.[57] Furthermore, for both systems the universality of the transition from quasiperiodicity to chaos had been determined quantitatively by the study of its multifractal character.[19,58]

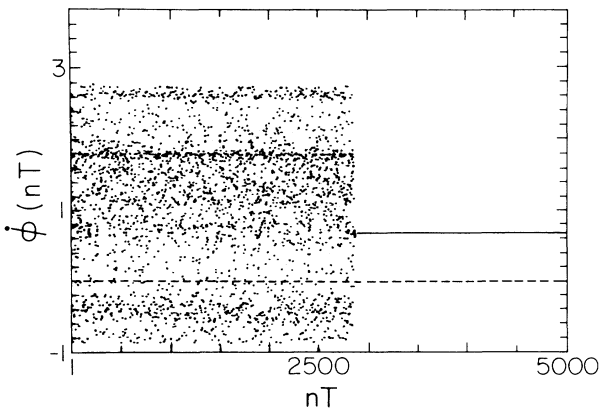

FIG. 13. Fluxon annihilation as a boundary crisis ($\rho=0.8$). Strobed time series $\phi_t(nT)$ vs nT presents a long chaotic transient.

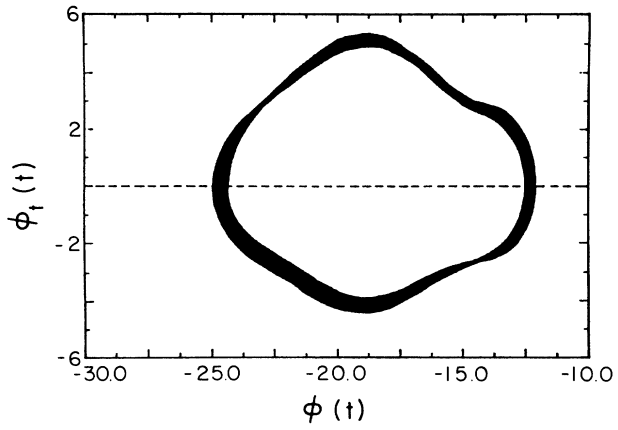

FIG. 14. Quasiperiodic regime ($\rho=2.625$). Phase space ϕ_t vs $\phi(t)$ reveals a trapped quasiperiodic solution in three wells of the periodic potential.

C. Spatiotemporal chaos

The existence and definition of the spatial chaos are problems that arise when attempting to extend the study of chaos to systems with many degrees of freedom and to continuous systems. Whereas temporal chaos is well understood and has a well-defined framework, the concept of spatial chaos is not clearly defined yet and often appears confused or mixed with disorder and turbulence.

We propose, alternatively, a definition of *spatiotemporal chaos* (rather than attempt to define merely spatial chaos) based on an extension of the concept of attractor in a dynamical scenario, i.e., the *spatiotemporal attractor.*

In the fluxonic regime the LJJ does not attain a complete spatiotemporal disorder; on the contrary, the dynamics are ruled by an attractor due to the alternate creation and destruction of fluxons in a sort of spatiotemporal analog of the stretching (due to the dissipation) and folding (due to the nonlinearity) process of the phase space that gives rise to a strange attractor in temporal chaos. Due to the active presence of the dissipation (fluxons can be annihilated when interacting between them or with the boundaries of the insulating barrier; these are radiative processes) and the nonlinearity (which creates the fluxons) in the process ruled by this spatiotemporal attractor, we consider as *spatiotemporal chaotic* the dynamics which involves a continuous formation and conversion of patterns.

The nonlinearity is a source of order that organizes solitonic patterns, both in the low-energy and the fluxonic regimes; this occurs in spite of the presence of nonconservative forces which do not allow the integrability of the equation and therefore precludes the existence of solitonic solutions. Curiously, the dissipation in this system also plays a role in the ordering of the dynamics, not only during the transients, but in the radiative collisions that give rise to the higher-energy breather states that alternate with the fluxonic windows.

Then, as a paradox, the dissipation acts in a contradictory way in the LJJ: it is a source of disorder (it can affect the integrability and therefore the existence of solitonic excitations) as well as behaves as a source of order (it plays an important role in the formation of solitonic patterns of the breather type) of the spatiotemporal dynamics.

V. SUMMARY AND CONCLUSIONS

We have shown that in in a LJJ, temporal chaos and solitons not only coexist but coalesce, giving rise to a new spatiotemporal phenomena with a very definite physical meaning.

In this regard, we have presented in this paper for the first time three distinct intermittency phenomena (intermittency induced by interior crises, spatiotemporal intermittency between strange attractors, and tangentlike spatiotemporal intermittency), all of them in the absence of noise, neither extrinsic to the system nor $(1/f)^d$-like noise induced by the system itself. This study contrasts with the accepted association of the hopping between dynamical attractors and $(1/f)^d$-like noise.[28,43–47] Many of the studies that sustained that association have had the junction without spatial extent as a scenario; this contrasts with the qualitatively different results that we have obtained for the LJJ.

The qualitative differences of our results for the LJJ are mainly due to the ability of the system to generate breatherlike excitations either below or above the fluxonic threshold. These solutions are trapped in one or more wells of the periodic potential, and their existence supposes the absence of a periodic voltage in the junction.

We have also presented three distinct types of chaotic regimes in their relation to the formation and conversion of spatiotemporal patterns: we have successively presented the chaotic oscillation of a solitonic structure of the breather type, intermittent chaos with alternate loss, and recovery of the solitonic character; and finally, spatiotemporal chaos in the presence of fluxons and noncoherent excitations.

We emphasized the appealing similarity, both qualitative and quantitative, of a variety of phenomena (which involves pattern formation and conversion, low-dimensional chaos, and spontaneously generated quasiperiodicity) which occur in both the LJJ and the Rayleigh-Bénard system; a pair of nonlinear, continuous, and dissipative systems. In fact, the Rayleigh-Bénard system appears as the hydrodynamical analog of the LJJ. This similar behavior suggests that the phenomenon of turbulence can be understood via the study of the transition from a few effective degrees of freedom to a high number of effective degrees of freedom[59] of the LJJ.

ACKNOWLEDGMENTS

The authors would like to acknowledge Dr. Juan Aponte for a critical reading of this manuscript. This work has been supported by Consejo Nacional de Investigaciones Científicas y Tecnológicas under Project No. S1-1828.

[1]See, for example, Proceedings of the Conference on Solitons and Coherent Structures, Santa Bárbara [Physica D **18**, 1 (1986)]; Proceedings of the Workshop on Spatio-Temporal Coherence and Chaos in Physical Systems, Los Alamos [Physica D **23**, 1 (1986)].

[2]K. Kaneko, *Collapse of Tori and Genesis of Chaos in Dissipative Systems* (World Scientific, Singapore, 1986), and references therein.

[3]J. P. Gollub and S. V. Benson, J. Fluid Mech. **100**, 449 (1980).

[4]P. R. Fenstermacher, H. L. Swinney, and J. P. Gollub, J. Fluid Mech. **94**, 103 (1979); V. S. V'vov, A. A. Predtechenskii, and A. I. Chernykh, Zh. Eksp. Teor. Fiz. **80**, 1099 (1981) [Sov. Phys.—JETP **53**, 562 (1981)].

[5]J. C. Eilbeck, P. S. Lomdahl, and A. C. Newell, Phys. Lett. A **87**, 1 (1981).

[6]D. Bennet, A. R. Bishop, and S. E. Trullinger, Z. Phys. B **47**, 265 (1982).

[7]K. Nozaki, Phys. Rev. Lett. **49**, 1883 (1982).

[8]A. R. Bishop, K. Fesser, P. S. Lomdahl, and S. E. Trullinger, Physica D **7**, 259 (1983).

[9]A. R. Bishop, K. Fesser, P. S. Lomdahl, W. C. Kerr, M. B. Williams, and S. E. Trullinger, Phys. Rev. Lett. **50**, 1095 (1983).

[10]M. Imada, J. Phys. Soc. Jpn. **52**, 1946 (1983).

[11]F. K. Abdullaev and N. A. Khikmatov, Zh. Tekh. Fiz. **55**, 937 (1985) [Sov. Phys.—Tech. Phys. **30**, 561 (1985)].

[12]O. H. Olsen, P. S. Lomdahl, A. R. Bishop, and J. C. Eilbech, J. Phys. C **18**, L511 (1985).

[13]O. H. Olsen and M. R. Samuelsen, Appl. Phys. Lett. **47**, 1007 (1985).

[14]A. R. Bishop and P. S. Lomdahl, Physica D **18**, 54 (1986).

[15]A. R. Bishop, M. G. Forest, D. W. McLaughlin, and E. A. Overman II, Physica D **23**, 293 (1986).

[16]A. R. Bishop, Helv. Phys. Acta **59**, 811 (1986).

[17]M. Cirillo, J. Appl. Phys. **60**, 338 (1986).

[18]O. H. Olsen and M. R. Samuelsen, Phys. Lett. A **119**, 391 (1987).

[19]L. E. Guerrero and M. Octavio, Jpn. J. Appl. Phys. **S26-3**, 1641 (1987); Phys. Rev. A **37**, 3641 (1988).

[20]A. R. Bishop, D. W. McLaughlin, M. G. Forest, and E. A. Overman II, Phys. Lett. A **127**, 335 (1988).

[21]A. Barone, F. Esposito, C. J. Magee, and A. C. Scott, Riv. Nuovo Cimento **1**, 227 (1971), and references therein; A. R. Bishop, J. A. Krumhansl, and S. E. Trullinger, Physica D **1**, 1 (1980), and references therein.

[22]A. Fujimaki, K. Nakajima, and Y. Sawada, Phys. Rev. Lett. **59**, 2895 (1987).

[23]M. Octavio, Phys. Rev. B **29**, 1231 (1984).

[24]A. C. Scott, F. Chu, and S. Reible, J. Appl. Phys. **47**, 3272 (1976).

[25]A. Barone and G. Paterno, *Physics and Applications of the Josephson Effect* (Wiley, New York, 1982), Chaps. 1 and 10.

[26]C. Grebogi, E. Ott, and J. A. Yorke, and Phys. Rev. Lett. **48**, 1507 (1982); Physica D **7**, 181 (1983).

[27]H. Bai-Lin, *Chaos* (World Scientific, Singapore, 1984), Chap. 4.

[28]E. G. Gwinn and R. M. Westervelt, Phys. Rev. A **33**, 4143 (1986).

[29]E. G. Gwinn and R. M. Westervelt, Phys. Rev. Lett. **54**, 1613 (1985).

[30]K. Sakai and Y. Yamaguchi, Phys. Rev. B **30**, 1219 (1984).

[31]R. L. Kautz and J. C. Macfarlane, Phys. Rev. A **33**, 498 (1986).

[32]H. Chaté and P. Manneville, Phys. Rev. A **32**, 3065 (1985).

[33]Y. H. Kao, J. C. Huang, and Y. S. Gou, Phys. Rev. A **34**, 1628 (1986).

[34]R. L. Kautz, J. Appl. Phys. **62**, 198 (1987).

[35]C. Jeffries and J. Pérez, Phys. Rev. A **27**, 601 (1983).

[36]H. Ikezi, J. S. deGrassie, and T. H. Jensen, Phys. Rev. A **28**, 1207 (1983).

[37]R. W. Rollins and E. R. Hunt, Phys. Rev. A **29**, 3327 (1984).

[38]R. Hilborn, Phys. Rev. A **31**, 378 (1985).

[39]R. Van Buskirk and C. Jeffries, Phys. Rev. A **31**, 3332 (1985).

[40]E. R. Hunt and R. W. Rollins, Phys. Rev. A **29**, 1000 (1984).

[41]R. W. Rollins and E. R. Hunt, Phys. Rev. Lett. **49**, 1295 (1982).

[42]M. Octavio, A. DaCosta, and J. Aponte, Phys. Rev. A **34**, 1512 (1986).

[43]S. M. Rezende, O. F. de Alcantara Bonfim, and F. M. de Aguiar, Phys. Rev. B **33**, 5153 (1986).

[44]H. G. Schuster, *Deterministic Chaos* (Physik-Verlag, Weinheim, 1984), p. 79ff.

[45]F. T. Arecchi, R. Meucci, G. Puccioni, and J. Tredicce, Phys. Rev. Lett. **49**, 1217 (1982).

[46]F. T. Arecchi, R. Badii, and A. Politi, Phys. Rev. A **29**, 1006 (1984).

[47]F. T. Arecchi, R. Badii, and A. Politi, Phys. Rev. A **32**, 402 (1985).

[48]H. T. Moon and M. V. Goldman, Phys. Rev. Lett. **53**, 1821 (1984).

[49]H. Chaté and P. Manneville, Phys. Rev. Lett. **58**, 112 (1987).

[50]S. Ciliberto and P. Bigazzi, Phys. Rev. Lett. **60**, 286 (1988).

[51]V. I. Karpman, Phys. Lett. A **88**, 207 (1982).

[52]B. Dueholm, E. Joergensen, O. A. Levring, J. Mygind, N. F. Pedersen, M. R. Samuelsen, O. H. Olsen, and M. Cirillo, Physica B **108**, 1303 (1981).

[53]O. A. Levring, M. Cirillo, B. Dueholm, E. Joergensen, J. Mygind, O. H. Olsen, N. F. Pedersen, M. R. Samuelsen, and O. H. Soerensen, Phys. Scr. **25**, 910 (1982).

[54]S. Ciliberto and M. A. Rubio, Phys. Rev. Lett. **58**, 2652 (1987).

[55]Yu. S. Kivshar' and B. A. Malomed, Zh. Eksp. Teor. Fiz. **90**, 2162 (1986) [Sov. Phys.—JETP **63**, 1267 (1986)], and references therein.

[56]R. L. Kautz, J. Appl. Phys. **58**, 424 (1985).

[57]J. Stavans, F. Heslot, and A. Libchaber, Phys. Rev. Lett. **55**, 596 (1985); A. P. Fein, M. S. Heutmaker, and J. P. Gollub, Phys. Scr. **T9**, 79 (1985).

[58]M. H. Jensen, J. P. Kadanoff, A. Libchaber, I. Procaccia, and J. Stavans, Phys. Rev. Lett. **55**, 2798 (1985).

[59]C. Tang, K. Wiesenfeld, P. Bak, S. Coppersmith, and P. Littlewood, Phys. Rev. Lett. **58**, 1161 (1987).